Hybrid Lightwave/RF Cooperative NOMA Networks

Yue Xiao, Panagiotis D. Diamantoulakis, *Senior Member, IEEE,* Zequn Fang, Zheng Ma, *Member, IEEE,* Li Hao, *Member, IEEE* and George K. Karagiannidis, *Fellow, IEEE*

***Abstract*—We propose an indoor lightwave downlink wireless communication network with the non-orthogonal multiple access (NOMA) technology, that consists of one visible light communication (VLC) access point (AP) and a pair of randomly located users. Although both users can directly receive information from the AP, the performance of the far user is degraded compared to the near one due to the asymmetrical channel gains. Thus, the user cooperation strategy is proposed to improve the performance of the far user by using mixed VLC/RF relaying technique in parallel with the wireless optical direct link. To efficiently exploit the available heterogeneous links, the concept of cross-band selection combining (CBSC) is introduced, according to which the far user is continuously served by either the mixed VLC/RF or the direct VLC link. Meanwhile, the performance of the proposed scheme is thoroughly investigated and compared to appropriate baselines. To this end, we derive closed-form expressions for the outage probability of each user as well as the system sum throughput. Finally, simulation results are provided to verify the effectiveness of the proposed scheme and the accuracy of the corresponding analysis.**

***Index Terms*—Lightwave, hybrid system, decode-and-forward relaying, non-orthogonal multiple access (NOMA), cross band selection combining (CBSC).**

I. Introduction

THE main challenge to meet the ever-growing demands for high connectivity, reliability and data rates in the fifth generation (5G) of communication networks and beyond, is the saturation of the radio frequency (RF) spectrum. This problem, if not properly addressed, can create a bottleneck in the performance of future wireless networks, the development of novel applications as well as the potential profits of the communications service providers. In order to deal with the aforementioned challenges, the integration of optical spectrum in the design of wireless communication systems has been considered as a promising direction to deal with the spectrum scarcity problem. Consequently, the effective utilization of wireless technologies that operate across RF and optical spectrum bands under a *cross-band design* in the PHY and MAC layers is of paramount importance, with the aim to increase not only the available spectrum but also the overall spectral efficiency.

This work was supported by the National Natural Science Foundation of China (no. U1734209, no. U1709219, no. 61571373), Key International Cooperation Project of Sichuan Province (no. 2017HH0002), Marie Curie Fellowship (no. 796426), and NSFC China-Swedish project (no. 6161101297) and 111 project (No.111-2-14). The work of Y.Xiao was also supported by the CSC Programme.

Y. Xiao, Z.Fang, Z. Ma, and L. Hao are with the Provincial Key Lab of Information Coding and Transmission, Southwest Jiaotong University, Chengdu 610031, China (e-mails: alice_xiaoyue@hotmail.com ; fangzequn@my.swjtu.edu.cn; {zma, lhao}@home.swjtu.edu.cn).

P. D. Diamantoulakis and George K. Karagiannidis are with the Electrical and Computer Engineering Department, Aristotle University of Thessaloniki, Thessaloniki 54124, Greece, and also with the Provincial Key Lab of Information Coding and Transmission, Southwest Jiaotong University, Chengdu 610031, China (e-mails:{padiaman, geokarag}@auth.gr).

A. State-of-the-Art and Motivation

Visible light communication (VLC) occupies the frequency range from 400 THz to 800 THz, while RF holds the spectrum from 3 KHz to 300 GHz [1], [2]. VLC has recently attracted both academic and industrial interest, due to the inherent advantages of optical communication systems [1]–[6], as well as the adoption of the easy-to-modulate light emitting diodes (LEDs) in common lighting applications, which enables the utilization of existing lighting infrastructure for communication purposes. With the two-fold exploitation of LEDs-based systems, a vast amount of unused electromagnetic spectrum in the visible light region is enabled, which can be used to offer very high data rate and multi-connectivity. Moreover, by confining light into a limited space and referring to the aforementioned features, the realization of VLC system can substantially contribute to the emerging trends in communication systems. More specifically, it can provide enhanced security service, easy bandwidth reuse, increased energy efficiency and considerable energy savings, along with the immunity to RF interference, without contributing to RF contamination, etc. Due to these advantages, VLC has been recognized as a promising alternative/complementary technology to RF and envisioned to be one of the potential candidate technologies in the 5G Public-Private-Partnership (PPP) project, with the aim to facilitate wireless access to devices, especially in indoor applications [7]. However, the main challenges of VLC include users' mobility, as well as the mitigation ability of severe channel degradation at the absence of a strong direct link [8]. A promising direction to overcome these challenges is the utilization of hybrid VLC/RF systems [9]–[13], where RF and VLC are employed in parallel in order to extend the coverage and increase the quality-of-service (QoS) of VLC systems.

On the other hand, connectivity and spectral efficiency, which are the major objectives of the proposed cross-band design, can be increased through the use of non-orthogonal multiple access (NOMA) [14]. It is noted that NOMA has already been approved as a study item of the 3-rd Generation Partnership Project (3GPP) in Release 15 [15]. According to NOMA, multiple users' messages can be superposed on the power domain, while the successive interference cancellation

(SIC) can be adopted at the receiver side to distinguish the desired signals for each user [16]. One of the major challenges in power-domain NOMA is the fairness-aware resource allocation among users in order to strengthen the transmission reliability for the user who suffers from weaker channel conditions and/or stronger interference [17]–[21]. NOMA protocol has also been recently investigated in the context of VLC communications networks [22]–[25]. More specifically, to enhance spectral efficiency and fairness in the NOMA-VLC systems, a gain ratio power allocation has been proposed in [22], while the impact of user paring in NOMA VLC networks has been studied in [13], [23], [24].

In addition, mixed optical/RF relaying systems have also recently attracted the research interest [26]–[33]. Similarly to conventional RF relaying technique [34]–[37], the use of a VLC/RF relay improves the system performance in terms of capacity and/or coverage, with the additional benefit of easier full-duplex implementation, due the non-interfering nature of optical and RF technologies. Moreover, it is commonly assumed that the relay is a user of the network, i.e., it receives and forwards another user's messages voluntarily for the common purpose. Based on this assumption, VLC/RF relaying has been investigated in [26] considering a near-far user setup, in which the VLC access point (AP) simultaneously transmits both users' messages using the superposition coding (SC) technique. Assuming that the far user is out of the coverage of the VLC system, it receives its message solely via the near user, which acts as an RF relay. In this work, SC technique is used in a point-to-point communication, i.e., between the VLC AP and the near user, and thus, it does not offer any gain compared to the time-division multiplexing (TDM) technology in terms of channel capacity. On the other hand, as it has been shown in [38], SC technology outperforms time-division multiple access (TDMA) in the broadcast channels which have asymmetric gains. Moreover, in [27], [28], a dual-hop mixed VLC/RF cooperative system with simultaneous lightwave information and power transfer (SLIPT) [29], [39], [40] has been investigated. Although the utilization of SLIPT is out of the scope of this work, it deserves to be mentioned that it can further facilitate the user cooperation, since, in this case, the relay can solely consume the harvested energy to retransmit the received message. Furthermore, mixed free-space optical (FSO)/RF relaying systems with the use of decode-and-forward (DF) and amplify-and-forward (AF) schemes have been introduced in [32] and [33], respectively, while the secrecy performance in mixed FSO/RF relaying systems has been investigated in [30], [31]. However, to the best of our knowledge, the combined use of direct optical links and mixed optical/RF relaying links to serve the same user has not been investigated yet in the existing literature.

B. Contribution

Motivated by the advantages and vulnerabilities of the aforementioned technologies, i.e., RF, VLC, relaying and NOMA, this paper focuses on the design of a downlink hybrid VLC/RF relaying network with NOMA in a two-user scenario. Specifically, the VLC is used to provide access to both users, while the RF technology is solely used as a complementary technology to reduce the outage probability for the far user, by forwarding another copy of its message from the near user. Consequently, in contrast to [26], we assume that the far user receives two copies of its message, one from the VLC AP and one from the near user via RF. Moreover, in contrast to [26], we also consider the randomness of the users' locations. Furthermore, we derive closed-form expressions for the achievable rate, taking into account the VLC particularities, according to which VLC signals are non-negative and constrained by the desired illumination [38].

More specifically, the contributions of this work can be summarized as follows:

- We introduce the cross-band selection combining (CBSC) concept in a two-user hybrid VLC/RF relaying network with NOMA, according to which the far user adaptively chooses to decode the information from either the mixed VLC/RF link or the direct VLC link, based on the achievable rate and the required user's QoS on each of the links. For the sake of comparison, two fixed policies are used as baselines, according to which the far user is continuously served by either the mixed VLC/RF or the direct VLC link.
- We derive closed-form expressions for the user outage probability for all suggested policies, i.e., the CBSC and the two fixed ones. To obtain more insights on the outage performance of CBSC, upper and lower bounds are also derived.
- We derive a closed-form expression for the system sum throughput for all suggested policies to quantify the data rate of successful message delivery to both users.
- Finally, Monte-Carlo simulation results are provided to verify the effectiveness of the proposed scheme and the accuracy of the analysis. Specifically, it is shown that CBSC can obtain better outage performance and higher system sum throughput, in contrast to the fixed policies. Additionally, it becomes evident from the simulation results, that the proposed analysis can be used to optimize the system's parameters, such as the semi-angle of illumination, the vertical distance of the VLC AP, and the users' power allocation at the VLC AP.

C. Structure

The rest of the paper is structured as follows. The system model for hybrid VLC/RF cooperative relaying is introduced in Section II. In Section III, the users' outage probability and system throughput, for the fixed policies, i.e., the mixed VLC/RF policy and the direct VLC policy, are derived, respectively. The corresponding performance analysis for the proposed CBSC policy is investigated in Section IV, where the upper and lower bounds for the outage probability are also illustrated. Simulation results are given and discussed in V. Finally, conclusions are summarized in Section VI.

II. System model

We consider an indoor downlink transmission system as presented in Fig. 1, where a VLC AP is placed on the ceiling,

The final version of record is available at http://dx.doi.org/10.1109/TWC.2019.2951401

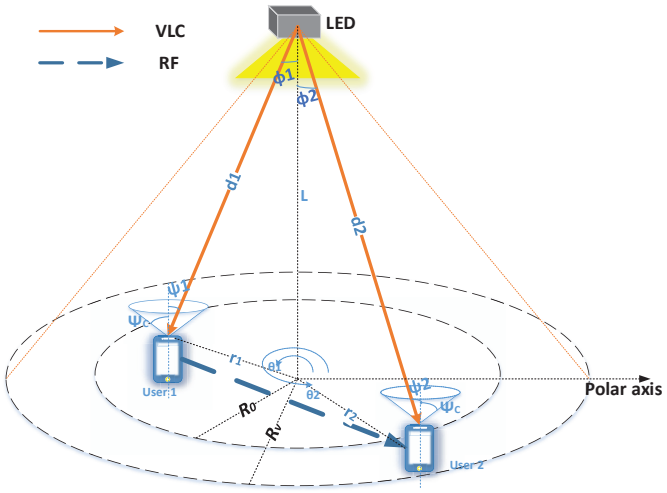

Fig. 1. System model of two-hop NOMA downlink relaying system.

with vertical distance L from the ground floor plane. For the sake of the analysis and without loss of generality, two types of users are considered, namely the *near* and the *far* one, denoted by U_1 and U_2 respectively. It is assumed that the locations of U_1 and U_2 are uniformly distributed inside a circle with horizontal radius R_0 and an annular area bounded by radii R_0 and R_v ($R_0 < R_v$), respectively. Specifically, in polar coordinates, users' positions can be represented by (r_i, θ_i), with r_i and θ_i being the radial and angular coordinate from the fixed reference axis, respectively.

It is assumed that both users belong inside the coverage area of the VLC AP and they both receive their messages from the direct VLC links using NOMA. However, in order to assist the far user, the near user also acts as a relay, using mixed VLC/RF DF relaying protocol. Also, considering that VLC is transparent to the communication at the RF band, U_1 operates in full-duplex mode [41], [42], i.e., it simultaneously receives and transmits information. In practice, the received symbol by U_2 at the RF band is delayed by one timeslot, i.e, during timeslot j, U_2 receives the symbols $x_{2,j}$ and $x_{2,j-1}$ by the VLC AP and U_1, respectively. However, for a sufficiently high number of transmitted symbols, the impact of this delay on the system's performance is insignificant and can be ignored. Moreover, the timing synchronization for hybrid RF/FSO systems has already been discussed in [43].

In a practical deployment, it's not possible to consider instantaneous channel state information (CSI) due to the large CSI feedback latency [25]. Motivated by this, to reduce the overhead and complexity, the performance of the considered system is evaluated assuming that solely the statistical CSI is available at the transmitter. Subsequently, a fixed rate requirement is considered for each receiver, with Γ_1 and Γ_2 being the target rates for U_1 and U_2, respectively. In this case, the key performance metrics are the outage probability and system throughput.

A. VLC Transmission

By employing intensity modulation-direct detection (IM-DD) in the optical communication system, the light intensity modulator at the transmitter is used to perform the electrical-to-optical conversion, while the electrical current carrying the signal information can be retrieved from the received lightwave via a photo-detector. Moreover, due to its inherent characteristics, the operation of the VLC is subject to the following constraints [38], [44], [45]:

- non-negativity of input x_v: the input signal modulates the optical intensity of the emitted light, as a result, the input signal x_v is non-negative and proportional to the light intensity, while the photo-detector produces an output signal whose optical power is proportional to the detected intensity, corrupted by AWGN.
- peak optical power $\mathcal{A}$ and average optical power ξ constraints: In VLC systems, the control of the transmitted optical power is vital for safety reasons and/or for dimming control in order to satisfy the illumination requirements.

Based on the above assumptions, the non-negativity signal x_v transmitted from the VLC AP, which is the superposition of the desired signals that correspond to U_1 and U_2, respectively, and can be expressed as

$$x_v = x_1 + x_2. \tag{1}$$

In (1), x_1 and x_2 are the messages to the users U_1 and U_2, respectively. To satisfy the peak and average constraints mentioned above, we let $\mathcal{A}_1 = \beta_1\mathcal{A}$, $\mathcal{A}_2 = \beta_2\mathcal{A}$, and $\mathbb{E}(x_1) = \mathbb{E}(x_2) = \xi$, where $\mathbb{E}(\cdot)$ denotes expectation and $\mathcal{A}_i$ is the peak intensity constraints of $x_i (i \in \{1, 2\})$. Also, β_1 and β_2 are the corresponding power allocation values, which are subject to the constraints $\beta_1 + \beta_2 = 1$ and $\beta_2 > \beta_1$, to ensure user fairness in the utilized downlink NOMA protocol [46]. Furthermore, $\mathcal{A}$ and $\xi = \alpha\mathcal{A}$ denote the peak and average illumination of the transmitted x_v respectively, where α is the corresponding illumination parameter with $\alpha \in [0, 1]$. Due to these constraints, the average illumination should satisfy

$$\beta_1\alpha\mathcal{A} + \beta_2\alpha\mathcal{A} = \xi. \tag{2}$$

Accordingly, at the user U_i ($i \in \{1, 2\}$), direct detection (DD) scheme is utilized to retrieve the electrical current from the received optical signal, thus, the corresponding received information can be expressed as

$$y_i = h_i\eta x_v + n_i, \tag{3}$$

with η being the photo-detector responsivity in A/W and n_i being the additive white Gaussian noise (AWGN). Also, h_i denotes the VLC channel gain from the VLC AP to the i-th user, which is given by [47]

$$h_i = \frac{(m+1)A_r}{2\pi d_i^2}\cos^m(\phi_i)T(\psi_i)g(\psi_i)\cos(\psi_i), \tag{4}$$

where A_r is the detector area of the i-th user, ϕ_i and ψ_i are the irradiance and incidence angles of the i-th user, respectively, and the Lambertian emission order m can be obtained by

$$m = -\ln 2/\ln(\cos\Phi_{1/2}), \tag{5}$$

with $\Phi_{1/2}$ being the transmitter semi-angle corresponding to the half illumination power. Moreover, $d_i = \sqrt{r_i^2 + L^2}$ denotes the distance between the VLC AP and the i-th user. Assuming that the optical detector of each user side is vertical to the horizontal plane, it holds that $\phi_i \approx \psi_i$. Besides, $T(\psi_i)$ and $g(\psi_i)$ are defined as the gains of the optical filter and optical concentrator, respectively. Moreover, the idealized gain of nonimaging optical concentrator is given by

$$g(\psi_i) = \begin{cases} \frac{n^2}{\sin^2 \Psi_C} & , 0 \le \psi_i \le \Psi_C \\ 0 & , \psi_i > \Psi_C, \end{cases} \tag{6}$$

where Ψ_C denotes the receiver's filed-of-view and n is the internal refractive index, which takes a typical value between 1 to 2 for visible light [47].

As it becomes evident from (4), h_i is directly affected by the distance between the VLC AP and i-th user. Also, recalling that U_1 and U_2 are assumed to be uniformly distributed in a disk of radius R_0 and an annular area bounded by $[R_0, R_v]$, respectively, the polar coordinates of each user (r_i, θ_i) follow the uniform distribution. The channel gain in (4) can easily be expressed as a function of the users' location, as in [23], i.e.,

$$\begin{aligned} h_i &= \frac{(m+1)A_r T(\psi_i) g(\psi_i)}{2\pi} \frac{L^{(m+1)}}{(r_i^2 + L^2)^{\frac{m+3}{2}}} \\ &= \frac{C(m+1)L^{(m+1)}}{(r_i^2 + L^2)^{\frac{m+3}{2}}}, \end{aligned} \tag{7}$$

where $C = \frac{A_r T(\psi_i) g(\psi_i)}{2\pi}$.

To derive the cumulative density function (CDF) of the channel power gains, we define $Y_i = |h_i|^2$, $Y_i \in [Y_{i,\min}, Y_{i,\max}]$, which receives its minimum and maximum value when the user is located at $r_{i,\min}$ and $r_{i,\max}$, respectively. Moreover, by plugging $r_1 \in [0, R_0]$ and $r_2 \in [R_0, R_v]$ into (7), the ranges for Y_1 and Y_2 can be written as

$$\begin{aligned} &[Y_{1,\min}, Y_{1,\max}] = \\ &\qquad \Big[\frac{(C(m+1)L^{(m+1)})^2}{(R_0^2 + L^2)^{(m+3)}}, \frac{(C(m+1)L^{(m+1)})^2}{L^{2(m+3)}}\Big], \\ &[Y_{2,\min}, Y_{2,\max}] = \\ &\qquad \Big[\frac{(C(m+1)L^{(m+1)})^2}{(R_v^2 + L^2)^{(m+3)}}, \frac{(C(m+1)L^{(m+1)})^2}{(R_0^2 + L^2)^{(m+3)}}\Big], \end{aligned} \tag{8}$$

respectively. Subsequently, the corresponding CDF of Y_i can be expressed as

$$\begin{aligned} F_{|h_i|^2}(y) &= \Pr\Big[\frac{(C(m+1)L^{(m+1)})^2}{(r_i^2 + L^2)^{m+3}} < y\Big] \\ &= 1 - \Pr\Big[r_i < T(y)\Big], \end{aligned} \tag{9}$$

where $T(y)$ is defined as

$$T(y) = \sqrt{\Big(\frac{(C(m+1)L^{(m+1)})^2}{y}\Big)^{\frac{1}{3+m}} - L^2}.$$

Recalling the assumption of uniform distribution and predefined locations for r_1 and r_2, the corresponding probability density functions (PDFs) can be written as [48]

$$f_{r_1}(d_1) = \frac{2d_1}{R_0^2}, \qquad 0 \le d_1 \le R_0, \tag{10}$$

and

$$f_{r_2}(d_2) = \frac{2(d_2 - R_0)}{(R_v - R_0)^2}, \qquad R_0 \le d_2 \le R_v, \tag{11}$$

respectively. Accordingly, the corresponding CDFs of the random radial variables r_1 and r_2 can be obtained by integrating (10) and (11) with respect to d_1 and d_2, respectively, which can be expressed as

$$F_{r_1}(d_1) = \int_0^{d_1} f_{r_1}(d_1) d_{d_1} = \frac{d_1^2}{R_0^2}, \qquad 0 \le d_1 \le R_0 \tag{12}$$

and

$$\begin{aligned} F_{r_2}(d_2) = \int_{R_0}^{d_2} f_{r_2}(d_2) d_{d_2} = \frac{d_2^2 + R_0^2 - 2R_0 d_2}{(R_v - R_0)^2}, \\ R_0 \le d_2 \le R_v. \end{aligned} \tag{13}$$

Consequently, the CDF of Y_i can be obtained by substituting (9) and (12) into (13), as

$$\begin{aligned} &F_{|h_1|^2}(y_1) = \\ &\begin{cases} 1 - \frac{T(y_1)^2}{R_0^2} & , Y_{1,\min} \le y_1 \le Y_{1,\max} \\ 1 & , y_1 > Y_{1,\max} \\ 0 & , y_1 < Y_{1,\min} \end{cases} \end{aligned} \tag{14}$$

and

$$\begin{aligned} &F_{|h_2|^2}(y_2) = \\ &\begin{cases} 1 - \frac{T(y_2)^2 - 2R_0 T(y_2) + R_0^2}{(R_v - R_0)^2} \\ \qquad\qquad , Y_{2,\min} \le y_2 \le Y_{2,\max} \\ 1 & , y_2 > Y_{2,\max} \\ 0 & , y_2 < Y_{2,\min}. \end{cases} \end{aligned} \tag{15}$$

Moreover, for VLC with IM-DD [38], [44], [45], the capacity cannot be described by the traditional Shannon formula, commonly used in RF systems, due to the constraints of the transmitted signal, i.e., non-negativity, peak and average illumination. Furthermore, in power domain NOMA, the stronger user, i.e., U_1, first decodes the message of the weaker user with rate $\mathcal{R}_{2\to1,V}$, and then obtains its own message with rate $\mathcal{R}_{1,V}$. On the other hand, the weaker user, i.e., U_2, decodes its own message with rate $\mathcal{R}_{2,V}$, by handling x_1 as interference. Due to SIC procedure in power domain NOMA, the desired information x_1 can be obtained at U_1 only after decoding the x_2 successfully. Considering all the above particularities of NOMA VLC systems and the received electrical signal given by (3), the achievable rates $\mathcal{R}_{2\to1,V}$, $\mathcal{R}_{1,V}$, and $\mathcal{R}_{2,V}$ can be described by the corresponding capacity lower bounds that have been derived in [38] and can be written as

$$\mathcal{R}_{2\to1,V} = \Big[B_v \log_2\big(1 + \frac{(\eta\beta_2)^2(\alpha\mathcal{A})^2|h_1|^2}{((\eta\beta_1)^2(\alpha\mathcal{A})^2|h_1|^2 + 9\sigma^2)(1+\epsilon_\mu)^2}\big) - \epsilon_\phi\Big]^+, \tag{16}$$

$$\mathcal{R}_{1,V} = \Big[B_v \log_2\big(1 + \frac{(\eta\beta_1)^2(\alpha\mathcal{A})^2|h_1|^2}{9\sigma^2(1+\epsilon_\mu)^2}\big) - \epsilon_\phi\Big]^+, \tag{17}$$

and

$$\mathcal{R}_{2,V} = \Big[B_v \log_2\big(1 + \frac{(\eta\beta_2)^2(\alpha\mathcal{A})^2|h_2|^2}{((\eta\beta_1)^2(\alpha\mathcal{A})^2|h_2|^2 + 9\sigma^2)(1+\epsilon_\mu)^2}\big) - \epsilon_\phi\Big]^+, \tag{18}$$

where B_v is the bandwidth of the VLC network, $[\cdot]^+ = \max(0,\cdot)$, $\epsilon_\phi = 0.016$, $\epsilon_\mu = 0.0015$, σ^2 is the noise variance [38].

B. RF transmission

The received signal by U_2 at the RF frequency band is

$$y_R = \sqrt{P_t} x_t h_R + n_R, \tag{19}$$

where P_t represents the available power at U_1 for retransmission, x_t is the transmit signal with normalized power, i.e., $\mathbb{E}(|x_t|^2) = 1$. Also, $h_R \sim \text{Nakagami}(K_n, d_R^{-v})$ is the RF channel gain between U_1 and U_2, which is modeled by the Nakagami-m fading channel, with K_n being the fading parameter. Moreover, a special case is expected when $K_n = 1$, which corresponds to Rayleigh fading. Furthermore, d_R is calculated by the Euclidean distance, as

$$d_R = \sqrt{r_1^2 + r_2^2 - 2r_1 r_2 \cos(\theta_2 - \theta_1)} \tag{20}$$

and v being the path loss parameter. Also, n_R is the AWGN noise at the RF receiver of U_2, with average power σ_R^2. Thus, according to Shannon capacity, the achievable data rate for the information transmission between U_1 and U_2 via the RF link is [14]

$$\mathcal{R}_{2,R} = B_r \log_2\left(1 + \frac{P_t \mid h_R \mid^2}{\sigma_R^2}\right), \tag{21}$$

with B_r being the bandwidth of the RF system.

III. Fixed Policies

In this section, two fixed baseline policies are investigated in terms of outage probability and system throughput, according to which either the VLC direct link or the cooperative RF link from U_1 to U_2 is continuously used for information decoding by U_2. Hereinafter, $\mathrm{P_r}[.]$ denotes the probability of an event.

A. VLC and RF cooperative link

This subsection focuses on the scenario that the superposition signal transmitted by the VLC AP is exploited solely by U_1, while U_2 only uses the signal transmitted from U_1 over the RF frequency band for information decoding. As one can easily observe, in this case, U_2 can successfully decode its message only if it is successfully decoded by U_1. Next, the outage probability for each user is defined and analyzed.

1) *Outage probability for U_1*: Assuming that Γ_i is the required threshold transmission rate of the desired message x_i for U_i, then the outage probability for U_1 is defined as the probability that the achievable rate of the desired x_1 at U_1 is smaller than its corresponding Γ_1, which also depends on the SIC procedure.

Theorem 1. *The outage probability for U_1 can be expressed in closed-from as*

$$\mathrm{P}^1_{\mathrm{O,VLC}} = \begin{cases} 1 - \frac{T(\zeta^*)^2}{R_0^2} & ,\gamma_2 < \frac{\beta_2^2}{\beta_1^2} \\ 1 & ,\text{otherwise}, \end{cases} \tag{22}$$

where

$$\gamma_i = (2^{(\Gamma_i+\epsilon_\phi)/B_v} - 1)(1+\epsilon_\mu)^2, \tag{23a}$$
$$\zeta^* = \min\{\max\{\zeta, Y_{1,min}\}, Y_{1,max}\}, \tag{23b}$$
$$\zeta = \max(\zeta_1, \zeta_2), \tag{23c}$$
$$\zeta_1 = \frac{9\gamma_1}{(\eta\beta_1)^2(\alpha\rho_v)^2}, \tag{23d}$$
$$\zeta_2 = \frac{9\gamma_2}{((\eta\beta_2)^2 - (\eta\beta_1)^2\gamma_2)(\alpha\rho_v)^2}, \tag{23e}$$

and $(\alpha\rho_v)^2 = (\frac{\alpha\mathcal{A}}{\sigma})^2$ denotes the average transmit signal-to-noise (SNR) from the VLC AP.

Proof. The outage probability for user U_1 is defined as

$$\begin{aligned}\mathrm{P}^1_{\mathrm{O,VLC}} &\overset{(a)}{=} \mathrm{P_r}[\mathcal{R}_{2\to1,\mathrm{V}} < \Gamma_2] + \\ &\qquad \mathrm{P_r}[\mathcal{R}_{2\to1,\mathrm{V}} > \Gamma_2, \mathcal{R}_{1,\mathrm{V}} < \Gamma_1] \\ &\overset{(b)}{=} 1 - \mathrm{P_r}[\mathcal{R}_{2\to1,\mathrm{V}} > \Gamma_2 \cap \mathcal{R}_{1,\mathrm{V}} > \Gamma_1],\end{aligned} \tag{24}$$

where step (a) follows from the fact that the desired x_1 can be received only after decoding x_2 successfully, which also can be expressed as the complementary event of successful decoding by using step (b). Next, by plugging (16) and (17) into above (24), $\mathrm{P}^1_{\mathrm{O,VLC}}$ can be deduced as

$$\mathrm{P}^1_{\mathrm{O,VLC}} = \begin{cases} F_{|h_1|^2}(\zeta^*) & ,\gamma_2 < \frac{\beta_2^2}{\beta_1^2} \\ 1 & ,\text{otherwise}. \end{cases} \tag{25}$$

Consequently, by substituting (14) into (25), we can obtain a closed-form expression as given in (22), which completes the proof. □

2) *Outage probability for U_2*: When the mixed VLC/RF relaying link is used, the outage probability for U_2 can be expressed as

$$\mathrm{P}^2_{\mathrm{O,VLC/RF}} = \mathrm{P_r}[\min\{\mathcal{R}_{2\to1,\mathrm{V}}, \mathcal{R}_{2,\mathrm{R}}\} < \Gamma_2]. \tag{26}$$

By considering the complementary event of the one in (26), the latter can be rewritten as

$$\begin{aligned}\mathrm{P}^2_{\mathrm{O,VLC/RF}} &= 1 - \mathrm{P_r}\left[\mathcal{R}_{2\to1,\mathrm{V}} > \Gamma_2 \cap \mathcal{R}_{2,\mathrm{R}} > \Gamma_2\right] \\ &\overset{(c)}{=} 1 - \mathrm{P_r}[\mathcal{R}_{2\to1,\mathrm{V}} > \Gamma_2]\mathrm{P_r}[\mathcal{R}_{2,\mathrm{R}} > \Gamma_2 \big| \mathcal{R}_{2\to1,\mathrm{V}} > \Gamma_2],\end{aligned} \tag{27}$$

where step (c) follows the concept of conditional probability and the fact that channels h_1 and h_R are not independent due to the impact of the users' locations on the quality of the RF link, according to (20). Then, by using similar steps as in the proof of Theorem 1, the following expression is derived:

$$\mathrm{P_r}[\mathcal{R}_{2\to1,V} > \Gamma_2] = \begin{cases} \mathrm{P_r}[r_1 < r_1^c] & ,\gamma_2 < \frac{\beta_2^2}{\beta_1^2} \\ 1 & ,\text{otherwise}, \end{cases} \tag{28}$$

where

$$r_1^c = \sqrt{\left(\frac{(C(m+1)L^{(m+1)})^2}{\zeta_{2,1}^*}\right)^{\frac{1}{3+m}} - L^2}, \tag{29}$$

and

$$\zeta_{2,1}^* = \min\{\max\{\zeta_2, Y_{1,min}\}, Y_{1,max}\}. \tag{30}$$

Next, by using the result of (28), the conditional probability of $[\mathcal{R}_{2,R} > \Gamma_2]$ given $[\mathcal{R}_{2\to 1,V} > \Gamma_2]$ in (27), can be calculated as

$$\begin{aligned}&\mathrm{P_r}[\mathcal{R}_{2,R} > \Gamma_2 \big| \mathcal{R}_{2\to 1,V} > \Gamma_2] \\ &= \mathrm{P_r}[\mathcal{R}_{2,R} > \Gamma_2 \big| r_1 < r_1^c] = \mathrm{P_r}\Big[|h_R|^2 > \frac{\gamma_R}{\rho_t} \big| r_1 < r_1^c\Big]\end{aligned} \tag{31}$$

where $\gamma_R = 2^{\Gamma_2/B_r} - 1$, $\rho_t = \frac{P_t}{\sigma_R^2}$ is the transmit SNR at U_1, and the distance d_R given in (20) with v being assumed as an even number, for mathematical tractability [49]. Under the assumption of Nakagami-m fading over the RF, i.e., h_R, with fading parameter K_n, the corresponding channel gain $|h_R|^2$ is gamma-distributed with shape K_n and scale $\frac{d_R^{-v}}{K_n}$, i.e., $|h_R|^2 \sim \mathrm{Gamma}(K_n, \frac{d_R^{-v}}{K_n})$. Accordingly, if K_n is a positive integer, (27) can be obtained as

$$\mathrm{P}^2_{\mathrm{O,VLC/RF}} = 1 - e^{-\frac{\gamma_R K_n}{d_R^{-v}\rho_t}} \sum_{j=0}^{K_n-1} \frac{(\frac{\gamma_R K_n}{d_R^{-v}\rho_t})^j}{j!}, \quad r_1 < r_1^c. \tag{32}$$

Moreover, by taking into account the randomness of users' locations, θ_i is also uniformly distributed in the interval $[0, 2\pi]$ and its PDF is given by $f_{\theta_i}(x) = \frac{1}{2\pi} (i \in \{1, 2\})$, thus, we rewrite (26) while considering the limited area given in (29), as

$$\mathrm{P}^2_{\mathrm{O,VLC/RF}} = 1 - \mathbb{E}\big[e^{-\frac{\gamma_R K_n}{d_R^{-v}\rho_t}} \sum_{j=0}^{K_n-1} \frac{(\frac{\gamma_R K_n}{d_R^{-v}\rho_t})^j}{j!}\big], \quad r_1 < r_1^c. \tag{33}$$

Theorem 2. *A closed-form expression in the high SNR regime for the outage probability for U_2 is*

$$\begin{aligned}&\mathrm{P}^2_{\mathrm{O,VLC/RF}} \\ &= \frac{(\frac{\gamma_R K_n}{\rho_t})^{K_n}}{\pi^2 R_0^2 (R_v - R_0)^2 K_n!} \sum_{k=0}^{vK_n/2} \binom{\frac{vK_n}{2}}{k} (-1)^{\frac{vK_n}{2}-k} J_1 J_2\end{aligned} \tag{34}$$

with

$$\begin{aligned}J_1 = &\sum_{q=0}^{vK_n/2-k} \binom{\frac{vK_n}{2}-k}{q} \Big[B(\frac{\frac{vK_n}{2}-k-q+1}{2}, \frac{q+1}{2}) \\ &\times \frac{(1+(-1)^{\frac{vK_n}{2}-k-q})(1+(-1)^q)}{2}\Big]^2 (-1)^{\frac{vK_n}{2}-k-q},\end{aligned} \tag{35}$$

where $B(x, y)$ is the beta function [50]. *Moreover, a closed-form expression of J_2 is given by*

$$\begin{aligned}J_2 = &2^{\frac{vK_n}{2}-k} \sum_{l=0}^{k} \binom{k}{l} \frac{1}{2l + \frac{vK_n}{2} - k + 2} (r_1^c)^{2l+\frac{vK_n}{2}-k+2} \\ &\times \Big[\frac{1}{k - 2l + \frac{vK_n}{2} + 2}(R_v^{k-2l+\frac{vK_n}{2}+2} - R_0^{k-2l+\frac{vK_n}{2}+2}) \\ &- \frac{R_0}{k - 2l + \frac{vK_n}{2} + 1}(R_v^{k-2l+\frac{vK_n}{2}+1} - R_0^{k-2l+\frac{vK_n}{2}+1})\Big].\end{aligned} \tag{36}$$

Proof. To obtain a closed-form expression, we consider the expectation operation in the above (34) in the high SNR regime, by using the approximation given in [51], thus we have

$$\begin{aligned}&e^{-\frac{\gamma_R K_n}{d_R^{-v}\rho_t}} \sum_{j=0}^{K_n-1} \frac{(\frac{\gamma_R K_n}{d_R^{-v}\rho_t})^j}{j!} \approx 1 - \frac{(\frac{\gamma_R K_n}{d_R^{-v}\rho_t})^{K_n}}{K_n!} \\ &\approx 1 - \frac{(\frac{\gamma_R K_n}{\rho_t})^{K_n}}{K_n!} \big(r_1^2 + r_2^2 - 2r_1 r_2 \cos(\theta_2 - \theta_1)\big)^{\frac{vK_n}{2}}\end{aligned} \tag{37}$$

As users are randomly deployed, it holds that

$$\begin{aligned}&\mathbb{E}\big[e^{-\frac{\gamma_R K_n}{d_R^{-v}\rho_t}} \sum_{j=0}^{K_n-1} \frac{(\frac{\gamma_R K_n}{d_R^{-v}\rho_t})^j}{j!}\big] \\ &\approx 1 - \frac{(\frac{\gamma_R K_n}{\rho_t})^{K_n}}{\pi^2 R_0^2 (R_v - R_0)^2 K_n!} \underbrace{\int_{R_0}^{R_v}\int_0^{r_1^c}\int_0^{2\pi}\int_0^{2\pi} (r_2 - R_0)}_{} \\ &\underbrace{r_1 \big(r_1^2 + r_2^2 - 2r_1 r_2 \cos(\theta_2 - \theta_1)\big)^{(vK_n/2)} d_{\theta_1} d_{\theta_2} d_{r_1} d_{r_2}}_{J}.\end{aligned} \tag{38}$$

While considering the independence of the variables (radius and angle) in the users' polar coordinates (r_i, θ_i), (38) can be further reduced into two separate double integrals, i.e., radial-based and angle-based integrals. Moreover, by applying binomial theorem, J in (38) can be rewritten as

$$\begin{aligned}J = &\sum_{k=0}^{vK_n/2} \binom{\frac{vK_n}{2}}{k} (-1)^{\frac{vK_n}{2}-k} \\ &\underbrace{\int_0^{2\pi}\int_0^{2\pi} \cos^{(\frac{vK_n}{2}-k)}(\theta_2 - \theta_1) d_{\theta_1} d_{\theta_2}}_{J_1} \\ &\underbrace{\int_{R_0}^{R_v}\int_0^{r_1^c} (r_1^2 + r_2^2)^k (2r_1 r_2)^{\frac{vK_n}{2}-k} r_1 (r_2 - R_0) d_{r_1} d_{r_2}}_{J_2},\end{aligned} \tag{39}$$

Considering Lemma 2 in [49], (35) can be derived by utilizing the equation (2.5.12.44) in [50] and the sum-difference formulas of trigonometric functions. Moreover, by considering the constrained areas of U_1 and U_2, we can evaluate the double-integral J_2 as

$$\begin{aligned}J_2 &= \int_{R_0}^{R_v}\int_0^{r_1^c} (r_1^2 + r_2^2)^k (2r_1 r_2)^{\frac{vK_n}{2}-k} r_1 (r_2 - R_0) d_{r_1} d_{r_2}, \\ &= 2^{\frac{vK_n}{2}-k} \sum_{l=0}^{k} \binom{k}{l} \int_0^{r_1^c} r_1^{(2l+\frac{vK_n}{2}-k+1)} d_{r_1} \times \\ &\quad \Big[\int_{R_0}^{R_v} r_2^{(k-2l+\frac{vK_n}{2}-1)} d_{r_2} - R_0 \int_{R_0}^{R_v} r_2^{(k-2l+\frac{vK_n}{2})} d_{r_2}\Big],\end{aligned} \tag{40}$$

from which (36) is derived.

By substituting (38), (39), (35) and (36) into (33), (34) is derived and the proof is completed. □

B. Direct VLC link

In this subsection, we investigate the policy according to which U_2 directly receives its message from the VLC AP, i.e., mixed VLC/RF relaying is never used.

Theorem 3. *When only the wireless optical link is used, the outage probability for U_2 can be expressed as*

$$\mathrm{P}^2_{\mathrm{O,VLC}} = \begin{cases} 1 - \frac{T(\zeta^*_{2,2})^2 - 2R_0T(\zeta^*_{2,2}) + R_0^2}{(R_v - R_0)^2} & ,\gamma_2 < \frac{\beta_2^2}{\beta_1^2} \\ 1 & ,\text{otherwise}, \end{cases} \tag{41}$$

where

$$\zeta^*_{2,2} = \min\{\max\{\zeta_2, Y_{2,min}\}, Y_{2,max}\}. \tag{42}$$

Proof. According to the decoding procedure, in this case holds that

$$\begin{aligned} \mathrm{P}^2_{\mathrm{O,VLC}} &= \mathrm{P_r}[\mathcal{R}_{2,\mathrm{V}} < \Gamma_2] \\ &= \begin{cases} F_{|h_2|^2}(\zeta^*_{2,2}) & ,\gamma_2 < \frac{\beta_2^2}{\beta_1^2} \\ 1 & ,\text{otherwise}. \end{cases} \end{aligned} \tag{43}$$

Then, a closed-form expression for the outage probability for U_2 can be obtained by using (15) and (43) and the proof is completed. □

C. System Sum Throughput

In order to characterize the successful message delivery over the communication channels, sum throughput is provided in this subsection, taking into account the predefined target rates Γ_i. The system sum throughput for the two fixed policies can be expressed by utilizing their corresponding outage probabilities, as

$$R_{VLC/RF} = (1 - \mathrm{P}^1_{\mathrm{O,VLC}})\Gamma_1 + (1 - \mathrm{P}^2_{\mathrm{O,VLC/RF}})\Gamma_2 \tag{44}$$

and

$$R_{VLC} = (1 - \mathrm{P}^1_{\mathrm{O,VLC}})\Gamma_1 + (1 - \mathrm{P}^2_{\mathrm{O,VLC}})\Gamma_2, \tag{45}$$

respectively, where the specific closed-form expressions of the outage probabilities (i.e., $\mathrm{P}^1_{\mathrm{O,VLC}}$, $\mathrm{P}^2_{\mathrm{O,VLC/RF}}$, $\mathrm{P}^2_{\mathrm{O,VLC}}$) have been provided in (22), (34) and (41).

IV. Cross-Band Selection Combining

A cross-band selection combining policy (CBSC) is introduced according to which U_2 uses the best from the two links, i.e., the mixed VLC/RF and the direct one, to decode its message. Consequently, CBSC is expected to reduce the outage probability for U_2 compared to the fixed policies presented in the previous section. CBSC is also motivated by the fact that although U_2 receives two copies of its message over the two bands, linear coherent combining technique (e.g., MRC) is not applicable to this scenario.

A. Outage Probability Analysis

When CBSC is used, the outage probability at U_2 is defined as the probability that the achievable rate at combiner output (both RF receiver and lightwave receiver) is lower than a predefined target rate [52]. Accordingly, the outage probability in this scheme can be determined by

$$\begin{aligned} \mathrm{P}^2_{\mathrm{O,CBSC}} &= \mathrm{P_r}[\mathcal{O}_2^{\mathrm{VLC}} \cap \mathcal{O}_2^{\mathrm{VLC+RF}}] \\ &= \mathrm{P_r}[\mathcal{O}_2^{\mathrm{VLC}}]\mathrm{P_r}[\mathcal{O}_2^{\mathrm{VLC/RF}} \big| \mathcal{O}_2^{\mathrm{VLC}}]. \end{aligned} \tag{46}$$

For simplicity and tractability, $\mathcal{O}_2^{VLC/RF}$ and $\mathcal{O}_2^{VLC}$ are denoted as the outage events of the message x_2 performing at the far user U_2, from the direct VLC link and the mixed VLC/RF relaying link, respectively.

In order to analyze the conditional probability in (46), we first define the probability of event $[\mathcal{O}_2^{\mathrm{VLC}}]$ as

$$\mathrm{P_r}[\mathcal{O}_2^{\mathrm{VLC}}] = \mathrm{P_r}[\mathcal{R}_{2,V} < \Gamma_2] = \mathrm{P_r}[r_2 > r_2^c], \tag{47}$$

where the constrained distance r_2^c of the far user is

$$r_2^c = \sqrt{\Big(\frac{(C(m+1)L^{(m+1)})^2}{\zeta^*_{2,2}}\Big)^{\frac{1}{3+m}} - L^2}. \tag{48}$$

Subsequently, the outage event $\mathcal{O}_2^{VLC/RF}$ can be decomposed into two cases: i) decoding x_2 at U_1 using VLC link is not successful; ii) x_2 can be decoded by U_1 correctly but outage occur due to the RF link from U_1 to U_2. Thus, the corresponding outage probability can be expressed as

$$\begin{aligned} \mathrm{P_r}[\mathcal{O}_2^{\mathrm{VLC/RF}}] &= \mathrm{P_r}[\mathcal{R}_{2\to1,\mathrm{V}} < \Gamma_2] \\ &\quad + \mathrm{P_r}[\mathcal{R}_{2,\mathrm{R}} < \Gamma_2 \big| \mathcal{R}_{2\to1,\mathrm{V}} > \Gamma_2] \\ &= \mathrm{P_r}[r_1 > r_1^c] + \mathrm{P_r}\big[|h_R|^2 < \frac{\gamma_R}{\rho_t} \big| r_1 < r_1^c\big]. \end{aligned} \tag{49}$$

Considering the above two outage events, we have

$$\begin{aligned} \mathrm{P_r}[\mathcal{O}_2^{\mathrm{VLC/RF}} \big| \mathcal{O}_2^{\mathrm{VLC}}] &= \mathrm{P_r}[r_1 > r_1^c, r_2 > r_2^c] \\ &\quad + \mathrm{P_r}\big[|h_R|^2 < \frac{\gamma_R}{\rho_t} \big| (r_1 < r_1^c, r_2 > r_2^c)\big]. \end{aligned} \tag{50}$$

Theorem 4. *While considering the randomness of users' locations, the outage probability for U_2 can be expressed in closed-form, as*

$$\begin{aligned} &\mathrm{P}^2_{\mathrm{O,CBSC}} \\ &= \frac{2(R_0^2 - (r_1^c)^2)}{R_0^2(R_v - R_0)^2}\Big(\frac{1}{2}R_v^2 - R_0R_v - \frac{1}{2}(r_2^c)^2 + R_0r_2^c\Big) + \\ &\frac{(\frac{\gamma_R K_n}{\rho_t})^{K_n}}{\pi^2 R_0^2(R_v - R_0)^2 K_n!} \sum_{k=0}^{vK_n/2} \binom{\frac{vK_n}{2}}{k} (-1)^{\frac{vK_n}{2}-k} J_1 J_{2,CBSC}, \end{aligned} \tag{51}$$

where J_1 is given in (35) and $J_{2,CBSC}$ can be expressed as

$$\begin{aligned} J_{2,CBSC} &= 2^{\frac{vK_n}{2}-k} \sum_{l=0}^{k} \binom{k}{l} \frac{(r_1^c)^{2l+\frac{vK_n}{2}-k+2}}{2l + \frac{vK_n}{2} - k + 2} \\ &\times \Big[\frac{1}{k - 2l + \frac{vK_n}{2} + 2}(R_v^{k-2l+\frac{vK_n}{2}+2} - (r_2^c)^{k-2l+\frac{vK_n}{2}+2}) \\ &- \frac{R_0}{k - 2l + \frac{vK_n}{2} + 1}(R_v^{k-2l+\frac{vK_n}{2}+1} - (r_2^c)^{k-2l+\frac{vK_n}{2}+1})\Big]. \end{aligned} \tag{52}$$

Proof. Considering the randomly deployed users in the constrained area, the average of the first term in (50) can be obtained as

$$\begin{aligned}&\mathrm{P_r}[r_1 > r_1^c, r_2 > r_2^c]\\&= \int_{r_2^c}^{R_v}\int_{r_1^c}^{R_0} \frac{2r_1}{R_0^2}\frac{2(r_2-R_0)}{(R_v-R_0)^2} d_{r_1} d_{r_2}\\&= \frac{2(R_0^2-(r_1^c)^2)}{R_0^2(R_v-R_0)^2}\Big(\frac{1}{2}R_v^2 - R_0R_v - \frac{1}{2}(r_2^c)^2 + R_0 r_2^c\Big).\end{aligned} \tag{53}$$

As for the second term in (50), the Euclidean distance between U_1 and U_2 through RF link in our system should also be taken into account, i.e., $d_R = \sqrt{r_1^2 + r_2^2 - 2r_1r_2\cos(\theta_2-\theta_1)}$, thus, we calculate the average outage probability by utilizing the users' polar coordinates, according to which

$$\begin{aligned}&\mathrm{P_r}\big[|h_R|^2 < \frac{\gamma_R}{\rho_t}\big|(r_1 < r_1^c, r_2 > r_2^c)\big]\\&\overset{(d)}{\approx} \frac{\gamma_R}{\rho_t(r_1^2+r_2^2-2r_1r_2\cos(\theta_2-\theta_1))^{(-vK_n/2)}}\\&= \frac{(\frac{\gamma_R K_n}{\rho_t})^{K_n}}{\pi^2 R_0^2(R_v-R_0)^2K_n!}\int_{r_2^c}^{R_v}\int_0^{r_1^c}\int_0^{2\pi}\int_0^{2\pi} r_1(r_2-R_0)\times\\&\big(r_1^2+r_2^2-2r_1r_2\cos(\theta_2-\theta_1)\big)^{(vK_n/2)} d_{\theta_1}\, d_{\theta_2}\, d_{r_1}\, d_{r_2},\end{aligned} \tag{54}$$

where step (d) follows from the high SNR approximation that given in (37). Then (54) can be further expressed as

$$\begin{aligned}&\mathrm{P_r}\big[|h_R|^2 < \frac{\gamma_R}{\rho_t}\big|(r_1 < r_1^c, r_2 > r_2^c)\big]\\&\approx \frac{(\frac{\gamma_R K_n}{\rho_t})^{K_n}}{\pi^2 R_0^2(R_v-R_0)^2K_n!}\sum_{k=0}^{vK_n/2}\binom{\frac{vK_n}{2}}{k}(-1)^{\frac{vK_n}{2}-k}\\&\quad\times\underbrace{\int_0^{2\pi}\int_0^{2\pi}\cos^{(\frac{vK_n}{2}-k)}(\theta_2-\theta_1)d_{\theta_1}d_{\theta_2}}_{J_1}\\&\quad\times\underbrace{\int_{r_2^c}^{R_v}\int_0^{r_1^c}(r_1^2+r_2^2)^k(2r_1r_2)^{\frac{vK_n}{2}-k}r_1(r_2-R_0)d_{r_1}d_{r_2}}_{J_{2,CBSC}},\end{aligned} \tag{55}$$

where a closed-form expression of J_1 is given in (35). Then, by recalling the procedure in (40) but with different constraints of the users' locations, i.e., $[0, r_1^c]$, $[r_2^c, R_v]$, $J_{2,CBSC}$ can be deduced as (52).

Finally, we can obtain the analytical expression for $\mathrm{P}^2_{\mathrm{O,CBSC}}$ by plugging (53) and (54) into (50), which completes the proof. □

B. Bounds on the Outage Probability

In order to intuitively figure out the behavior of the proposed CBSC method while reducing the computational complexity which is high due to the dependency of the direct and mixed VLC/RF links, following the upper and lower bounds are provided [53]. Specifically, the upper and lower bounds of $\mathrm{P_r}[\emptyset_2^{\mathrm{VLC}} \cap \emptyset_2^{\mathrm{VLC/RF}}]$ can be achieved by plugging (34) and (41) into the following expressions,

$$\mathrm{P}^{2,\mathrm{upp}}_{\mathrm{O,CBSC}} = \min\big(\mathrm{P_r}(\emptyset_2^{\mathrm{VLC}}), \mathrm{P_r}(\emptyset_2^{\mathrm{VLC/RF}})\big) \tag{56}$$

and

$$\mathrm{P}^{2,\mathrm{low}}_{\mathrm{O,CBSC}} = \mathrm{P_r}(\emptyset_2^{\mathrm{VLC}}) + \mathrm{P_r}(\emptyset_2^{\mathrm{VLC/RF}}) - 1, \tag{57}$$

respectively.

C. System Sum Throughput

Along with the outage probability analysis, the system sum throughput of this policy can be written as

$$R_{CBSC} = (1-\mathrm{P}^1_{\mathrm{O,VLC}})\Gamma_1 + (1-\mathrm{P}^2_{\mathrm{O,CBSC}})\Gamma_2, \tag{58}$$

where $\mathrm{P}^1_{\mathrm{O,VLC}}$ and $\mathrm{P}^2_{\mathrm{O,CBSC}}$ have already expressed in (22) and (51).

V. Simulations and Discussion

In this section, Monte Carlo simulations are performed to validate the proposed analytical framework and assess the impact of the VLC AP parameters (i.e., average transmit SNR, semi-angle, vertical height) and the users' power allocation (β_1, β_2) on the system's performance. Note that the value of the bandwidth for VLC is expressed with respect to the corresponding one for the RF. The values of all parameters are given in Table-I, if not otherwise specified. The performance

TABLE I
Simulation Parameters

Parameter	Value	Parameter	Value
R_0	1.5 m	v	2
R_v	3 m	A_r	1 cm^2
L	2.15 m	Ψ_C	60^o
n	1.5	$\Phi_{1/2}$	60^o
$T(\psi_i)$	1	η	0.5 A/W
B_v	$4B_r$		

metrics of the three policies (i.e., the two fixed that consider the direct VLC link only or the cooperative VLC-RF link to U_2 and the proposed CBSC) are investigated and compared. Hereinafter, to facilitate reading, "VLC", "Mixed VLC/RF relaying", and "Proposed CBSC" are used to refer to the aforementioned policies. Also, let Γ_i' denote the normalized rate requirement, i.e., $\Gamma_i' = \Gamma_i/B_r$.

Fig. 2 illustrates the outage probability of the three different policies versus the average SNR of the VLC AP, i.e., $(\alpha\rho_v)^2$, where the power allocation factors are set as $\beta_1 = 0.3, \beta_2 = 0.7$, and $\Gamma_1' = 2.2$ bits/s, $\Gamma_2' = 2.2$ bits/s. The comparison is performed for the two different SNR settings: $\rho_t = \frac{1}{3}(\alpha\rho_v)^2$ and fixed value of $\rho_t = 30$ dB, with different fading parameters assumed, i.e., K_n={1, 2}. Note that the RF transmission is employed in order to help the far user and therefore it makes sense to set the average SNR ρ_t lower than $(\alpha\rho_v)^2$, while considering the system fairness. Then, variable and constant transmit power at the RF link, ρ_t, are both considered to further investigate the impact of the RF link between U_1 and U_2 to the overall system's performance.

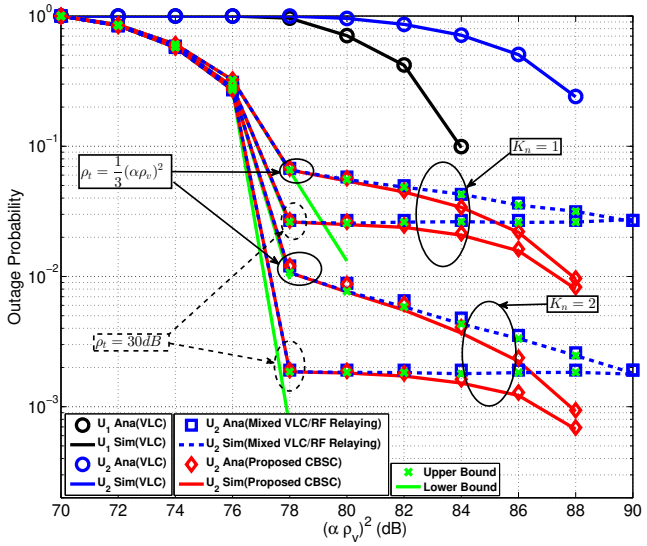

Fig. 2. Outage probability for different average transmit SNR from the VLC AP $(\alpha\rho_v)^2$.

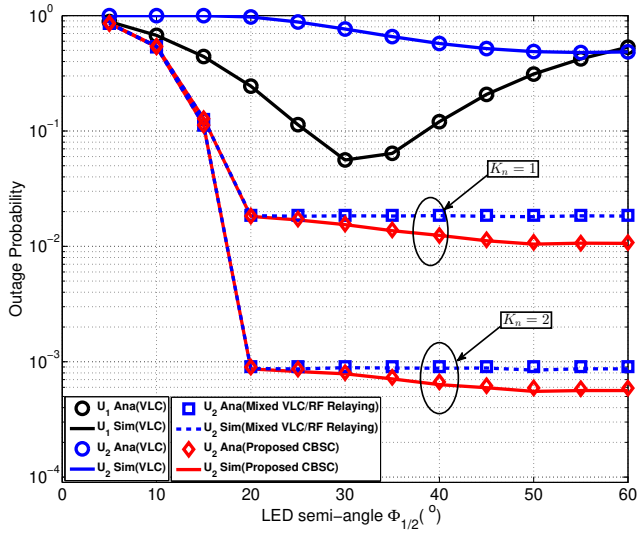

Fig. 3. Outage probability for different VLC AP semi-angle $\Phi_{1/2}$.

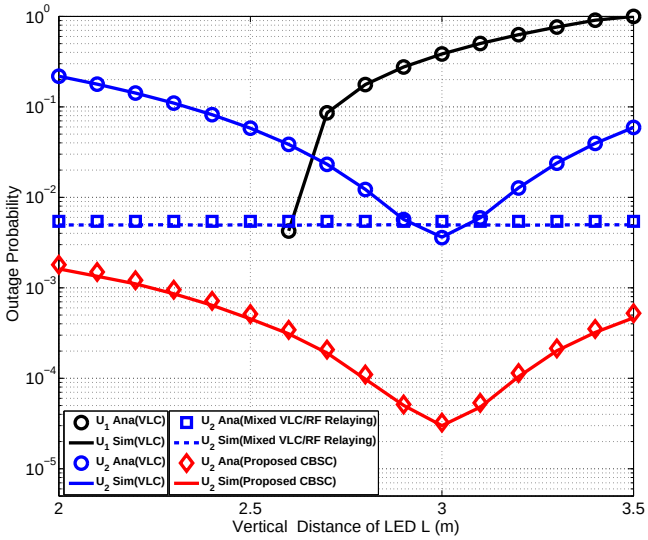

Fig. 4. Outage probability for different vertical height of the VLC AP.

Overall, the average outage probability of each user in the different policies decreases, when the SNR increases from 70 dB to 90 dB, except for the U_2 in cooperative VLC-RF link with $\rho_t = 30$ dB. This presents an error floor in the high SNR region, due to the constraint of fixed transmit power over the RF link. Compared with the above cases which consider only the direct VLC link, when the mixed VLC/RF relaying or the proposed CBSC policy are used, we focus on the outage probability for U_2. Additionally, as it is observed, both the mixed VLC/RF relaying and the proposed CBSC policy can be divided into two regions with different slopes. More specifically, since the direct VLC link to U_2 performs worse compared to the mixed VLC/RF relaying policy, the proposed CBSC is mainly affected by the mixed VLC/RF link. For this reason, the first region of the two policies are almost the same. On the other hand, with an increase of the average transmitted SNR from the VLC AP $(\alpha\rho_v)^2$, CBSC outperforms the mixed VLC/RF relaying policy. Additionally, the upper bound coincides with the cooperative VLC-RF link in this setup, which is in accordance with (56), while the lower bound is tight in the low SNR region.

The outage probabilities for each user in the above three policies are evaluated for several VLC AP semi-angles in Fig. 3, where the results can help to choose the proper value for the parameter. Furthermore, with $\beta_1 = 0.2, \beta_2 = 0.8$, $\Gamma_1' = 2.3$ bits/s, $\Gamma_2' = 2.3$ bits/s and $(\alpha\rho_v)^2 = 85$ dB, $\rho_t = 32$ dB, $K_n = \{1, 2\}$, the outage probability is illustrated versus the VLC AP semi-angle, which varies from 5^o to 60^o. For this configuration, it is notable that the outage probability for U_1 in the VLC link can acquire the optimal outage probability for the semi-angle value around 30^o.

Next, the outage probabilities are calculated for different realizations of the vertical distance of the VLC AP in Fig.4, which helps to figure out the optimum position of the VLC AP, with $K_n = 2$, $\beta_1 = 0.3, \beta_2 = 0.7$, $\Gamma_1' = 4.5$ bits/s, $\Gamma_2' = 2.82$ bits/s, $(\alpha\rho_v)^2 = 90$ dB, $\rho_t = 30$ dB. Regarding the impact of the AP's vertical distance on performance, an interesting observation is that setting $L = 3$ m minimizes the outage probability for U_2 when CBSC or the fixed direct VLC policy are utilized. However, the vertical distance of the VLC AP has no significant effect on the outage probabilities for U_2 when the mixed VLC/RF relaying is applied, due to the constant transmit power at the RF link. On the other hand, with the increase of the vertical distance of the VLC AP in the above settings, the outage probability for U_1 increases.

Furthermore, because of the power-domain NOMA protocol applied in this system, it's important to investigate the impact of the users' power allocation on the corresponding outage probabilities. In Fig. 5, we consider three different cases for the average transmit power, i.e., $(\alpha\rho_v)^2 = \{82, 85, 88\}$ dB and $\rho_t = 30$ dB, with $\Gamma_1' = 3.5$ bits/s, $\Gamma_2' = 3.5$ bits/s, and $K_n = 2$. As expected, the proposed CBSC performs better than the

The final version of record is available at http://dx.doi.org/10.1109/TWC.2019.2951401

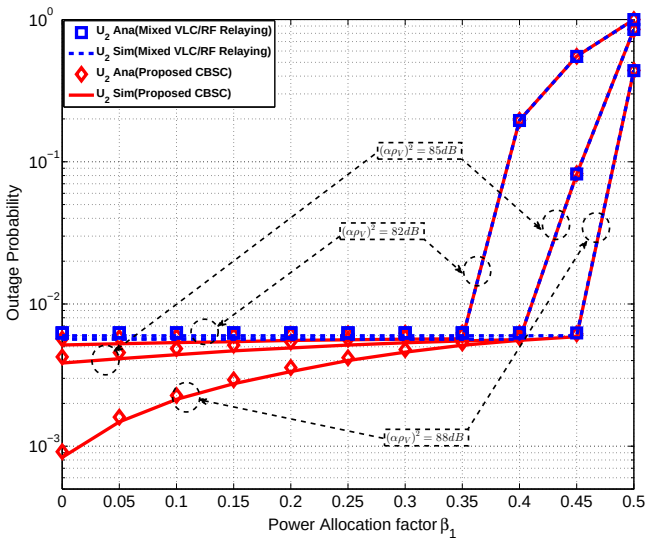

Fig. 5. Outage probability for different power allocation factors β_1.

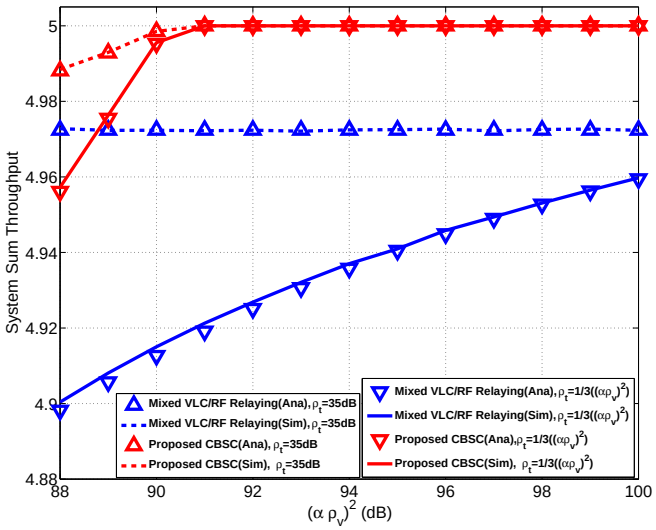

Fig. 6. System sum throughput for different average transmit SNR from the VLC AP.

mixed VLC/RF relaying, in terms of outage probability for U_2. However, as the transmit power at the VLC link increases and more power is allocated to β_1, the mixed VLC/RF relaying and CBSC asymptotically approach the same outage probability. This finding can be used to achieve a better performance by using proper power allocation. For example, when $(\alpha\rho_v)^2 = 82$ dB, the smallest power allocation leads to the same outage probability for U_2 in the mixed VLC/RF and the proposed CBSC is $\beta_1 = 0.35$, while $\beta_1 = \{0.4, 0.45\}$ corresponding to $(\alpha\rho_v)^2 = \{85, 88\}$ dB, respectively.

On the other hand, in Fig. 6, the system sum throughput is evaluated versus the average VLC AP transmit power $(\alpha\rho_v)^2$ in the range $[88 - 100]$ dB with fixed value, $\rho_t = 35$ dB or variables $\rho_t = \frac{1}{3}(\alpha\rho_v)^2$, $\Gamma_1' = 2.5$ bits/s, $\Gamma_2' = 2.5$ bits/s and $\beta_1 = 0.3, \beta_2 = 0.7$, $K_n = 2$. It is shown that the proposed CBSC is superior to the mixed VLC/RF relaying policy. Note that these results ignore the performance of the direct VLC policy, which is not competitive compared with the other two policies, i.e., the proposed CBSC and the mixed VLC/RF relaying. Furthermore, as the average SNR, i.e.,$(\alpha\rho_v)^2$, increases, the throughput of the proposed CBSC approaches the total target rate, i.e., 5 bits/s, in the high SNR region.

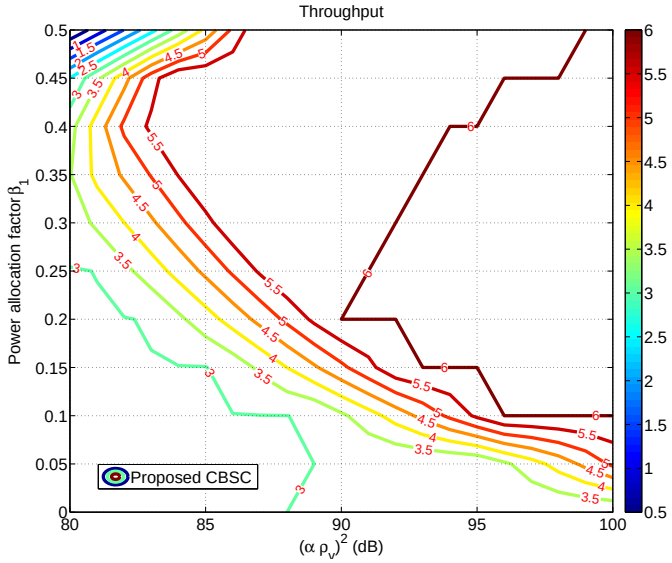

Fig. 7. Contour plot of system sum throughput versus power allocation β_1 and the average transmit SNR from the VLC AP.

In Fig. 7, the system throughput of the proposed CBSC is illustrated to further investigate the joint effect of the parameters, $(\alpha\rho_v)^2$ and β_1. We assume that the transmitted SNR for the RF link is $\rho_t = \frac{1}{3}(\alpha\rho_v)^2$ and target rates are $\Gamma_1' = 3$ bits/s, $\Gamma_2' = 3$ bits/s, with $K_n = 2$. By using the results in this figure, we can find the optimal parameter pair $(\beta_1^*, (\alpha\rho_v)^2)$, with the other VLC AP parameters fixed. Consequently, this figure can be used as a guide to achieve system performance.

VI. Conclusions

In this paper, we have introduced a novel cross-band selection combining (CBSC) method for a two-user hybrid lightwave/RF cooperative networks with NOMA, with the aim to improve the communication QoS for both users, as well as to extend the coverage of the network. According to CBSC, the far user adaptively chooses either the mixed VLC/RF relaying link or the direct VLC link to decode the information. In order to identify the performance of all the policies, closed-form expressions for the outage probability and the system sum throughput for the high SNR region were derived, taking into account the random locations of the near and far user. Moreover, upper and lower bounds for the outage probability of the proposed CBSC were presented. Furthermore, simulation results have been performed to verify the effectiveness of the proposed CBSC and the accuracy of the theoretical study. Specifically, it has been shown that the proposed CBSC offers significant improvement of the weaker user's outage probability and increases the system sum

throughput compared to the fixed policies. Finally, it is noted that in order to increase energy sustainability, the integration of SLIPT technology in hybrid lightwave/RF cooperative systems is a promising future direction.

REFERENCES

[1] D. Karunatilaka, F. Zafar, V. Kalavally, and R. Parthiban, "LED Based Indoor Visible Light Communications: State of the Art," *IEEE Commun. Surveys Tuts.*, vol. 17, no. 3, pp. 1649–1678, 2015.

[2] G. K. K. R. S. S. Arnon, J. R. Barry and E. M. Uysal, *Advanced Optical Wireless Communication Systems*. Cambridge, U.K.: Cambridge Univ. Press, 2012.

[3] A. M. Abdelhady, O. Amin, A. Chaaban, B. Shihada, and M. Alouini, "Downlink resource allocation for dynamic TDMA-based VLC systems," *IEEE Trans. Wireless Commun.*, pp. 1–1, 2018.

[4] M. Obeed, A. M. Salhab, M.-S. Alouini, and S. A. Zummo, "On Optimizing VLC Networks for Downlink Multi-User Transmission: A Survey," *arXiv:1808.05089*, 2018.

[5] Z. Liao, L. Yang, J. Chen, H. Yang, and M. Alouini, "Physical Layer Security For Dual-Hop VLC/RF Communication Systems," *IEEE Commun. Lett.*, pp. 1–1, 2018.

[6] M. Obeed, A. M. Salhab, S. A. Zummo, and M. Alouini, "Joint Optimization of Power Allocation and Load Balancing for Hybrid VLC/RF Networks," *IEEE J. Opt. Commun. Netw.*, vol. 10, no. 5, pp. 553–562, 2018.

[7] P. A. H. S. Zvanovec, P. Chvojka and Z. Ghassemlooy, "Visible Light Communications towards 5G," *Radioengineering*, vol. 24, no. 1, pp. 1–9, 2015.

[8] N. Chi, H. Haas, M. Kavehrad, T. D. C. Little, and X. Huang, "Visible Light Communications: Demand Factors, Benefits and Opportunities [Guest Editorial]," *IEEE Wireless Commun.*, vol. 22, no. 2, pp. 5–7, 2015.

[9] M. B. Rahaim, A. M. Vegni, and T. D. C. Little, "A Hybrid Radio Frequency and Broadcast Visible Light Communication System," in *Proc. IEEE GLOBECOM Workshops (GC Wkshps)*, 2011, pp. 792–796.

[10] M. O. O. A. M. Salhab, S. A. Zummo, and M. Alouini, "Joint Optimization of Power Allocation and Load Balancing for Hybrid VLC/RF Networks," *IEEE/OSA J. Opt. Commun. Netw.*, vol. 10, no. 5, pp. 553–562, 2018.

[11] E. S.-N. . M. Uysal, "Generalized Performance Analysis of Mixed RF/FSO Cooperative Systems," *IEEE Trans. Wireless Commun.*, vol. 15, no. 1, pp. 714–727, 2016.

[12] V. K. Papanikolaou, P. P. Bamidis, P. D. Diamantoulakis, and G. K. Karagiannidis, "Li-fi and wi-fi with common backhaul: Coordination and resource allocation," in *2018 IEEE Wireless Communications and Networking Conference (WCNC)*, Apr. 2018, pp. 1–6.

[13] V. K. Papanikolaou, P. D. Diamantoulakis, and G. K. Karagiannidis, "User grouping for hybrid vlc/rf networks with noma: A coalitional game approach," *IEEE Access*, pp. 1–1, 2019.

[14] X. Yue, Y. Liu, S. Kang, A. Nallanathan, and Z. Ding, "Exploiting Full/Half-Duplex User Relaying in NOMA Systems," *IEEE Trans. Commun.*, vol. 66, no. 2, pp. 560–575, 2018.

[15] *Study on Non-Orthogonal Multiple Access (NOMA) for NR*, 3GPP.

[16] Z. Ding, M. Peng, and H. V. Poor, "Cooperative Non-Orthogonal Multiple Access in 5G Systems," *IEEE Commun. Lett.*, vol. 19, no. 8, pp. 1462–1465, 2015.

[17] S. Timotheou and I. Krikidis, "Fairness for Non-Orthogonal Multiple Access in 5G Systems," *IEEE Signal Process. Lett.*, vol. 22, no. 10, pp. 1647–1651, 2015.

[18] P. D. Diamantoulakis and G. K. Karagiannidis, "Maximizing Proportional Fairness in Wireless Powered Communications," *IEEE Wireless Commun. Lett.*, vol. 6, no. 2, pp. 202–205, 2017.

[19] P. Xu and K. Cumanan, "Optimal Power Allocation Scheme for Non-Orthogonal Multiple Access With α -Fairness," *IEEE J. Sel. Areas Commun.*, vol. 35, no. 10, pp. 2357–2369, 2017.

[20] Y. Xiao, L. Hao, Z. Ma, Z. Ding, Z. Zhang, and P. Fan, "Forwarding Strategy Selection in Dual-Hop NOMA Relaying Systems," *IEEE Commun. Lett.*, vol. 22, no. 8, pp. 1644–1647, 2018.

[21] C. K. Vranas, P. S. Bouzinis, V. K. Papanikolaou, P. D. Diamantoulakis, and G. K. Karagiannidis, "On the Gain of NOMA in Wireless Powered Networks with Circuit Power Consumption," *IEEE Wireless Commun. Lett.*, pp. 1–1, 2019.

[22] H. Marshoud, V. M. Kapinas, G. K. Karagiannidis, and S. Muhaidat, "Non-Orthogonal Multiple Access for Visible Light Communications," *IEEE Photon. Technol. Lett.*, vol. 28, no. 1, pp. 51–54, 2016.

[23] L. Yin, W. O. Popoola, X. Wu, and H. Haas, "Performance Evaluation of Non-Orthogonal Multiple Access in Visible Light Communication," *IEEE Trans. Commun.*, vol. 64, no. 12, pp. 5162–5175, 2016.

[24] X. Zhang, Q. Gao, C. Gong, and Z. Xu, "User Grouping and Power Allocation for NOMA Visible Light Communication Multi-Cell Networks," *IEEE Commun. Lett.*, vol. 21, no. 4, pp. 777–780, 2017.

[25] H. Marshoud, P. C. Sofotasios, S. Muhaidat, G. K. Karagiannidis, and B. S. Sharif, "On the performance of visible light communication systems with non-orthogonal multiple access," *IEEE Transactions on Wireless Communications*, vol. 16, no. 10, pp. 6350–6364, Oct 2017.

[26] Y. Han, X. Zhou, L. Yang, and S. Li, "A Bipartite Matching Based User Pairing Scheme for Hybrid VLC-RF NOMA Systems," in *Proc.IEEE International Conference on Computing, Networking and Communications (ICNC)*, 2018, pp. 480–485.

[27] T. Rakia, H. Yang, F. Gebali, and M. Alouini, "Optimal Design of Dual-Hop VLC/RF Communication System With Energy Harvesting," *IEEE Commun. Lett.*, vol. 20, no. 10, pp. 1979–1982, 2016.

[28] M. R. Zenaidi, Z. Rezki, M. Abdallah, K. A. Qaraqe, and M. Alouini, "Achievable Rate-Region of VLC/RF Communications with an Energy Harvesting Relay," in *GLOBECOM 2017 - 2017 IEEE Global Communications Conference*, 2017, pp. 1–7.

[29] P. D. Diamantoulakis, G. K. Karagiannidis, and Z. Ding, "Simultaneous Lightwave Information and Power Transfer (SLIPT)," *IEEE Trans. Green Commun. and Netw.*, vol. 2, no. 3, pp. 764–773, 2018.

[30] H. Lei, Z. Dai, I. S. Ansari, K. Park, G. Pan, and M. Alouini, "On Secrecy Performance of Mixed RF-FSO Systems," *IEEE Photon. J.*, vol. 9, no. 4, pp. 1–14, 2017.

[31] J. Al-Khori, G. Nauryzbayev, M. M. Abdallah, and M. Hamdi, "Secrecy Performance of Decode-and-Forward Based Hybrid RF/VLC Relaying Systems," *IEEE Access*, vol. 7, pp. 10 844–10 856, 2019.

[32] S. Sharma, A. S. Madhukumar, S. R., and C. J. Sheng, "Performance Analysis of Hybrid FSO/RF Transmission for DF Relaying System," in *2017 IEEE Globecom Workshops (GC Wkshps)*, 2017, pp. 1–6.

[33] N. Cherif, I. Trigui, and S. Affes, "On the performance analysis of mixed multi-aperture FSO/multiuser RF relay systems with interference," in *2017 IEEE 18th International Workshop on Signal Processing Advances in Wireless Communications (SPAWC)*, 2017, pp. 1–5.

[34] D. S. Michalopoulos, A. S. Lioumpas, G. K. Karagiannidis, and R. Schober, "Selective cooperative relaying over time-varying channels," *IEEE Trans. Commun.*, vol. 58, no. 8, pp. 2402–2412, Aug. 2010.

[35] D. S. Michalopoulos and G. K. Karagiannidis, "Two-relay distributed switch and stay combining," *IEEE Trans. Commun.*, vol. 56, no. 11, pp. 1790–1794, Nov. 2008.

[36] ——, "Distributed Switch and Stay Combining (DSSC) with a Single Decode and Forward Relay," *IEEE Commun. Lett.*, vol. 11, no. 5, pp. 408–410, May 2007.

[37] Z. Chen, Z. Ding, X. Dai, and G. K. Karagiannidis, "On the Application of Quasi-Degradation to MISO-NOMA Downlink," *IEEE Trans. Signal Process.*, vol. 64, no. 23, pp. 6174–6189, Dec. 2016.

[38] A. Chaaban, Z. Rezki, and M. Alouini, "On the Capacity of the Intensity-Modulation Direct-Detection Optical Broadcast Channel," *IEEE Trans. Wireless Commun.*, vol. 15, no. 5, pp. 3114–3130, 2016.

[39] H. Tran, G. Kaddoum, P. D. Diamantoulakis, C. Abou-Rjeily, and G. K. Karagiannidis, "Ultra-small Cell Networks with Collaborative RF and Lightwave Power Transfer," *IEEE Trans. Commun.*, pp. 1–1, 2019.

[40] G. Pan, P. D. Diamantoulakis, Z. Ma, Z. Ding, and G. K. Karagiannidis, "Simultaneous lightwave information and power transfer: Policies, techniques, and future directions," *IEEE Access*, vol. 7, pp. 28 250–28 257, 2019.

[41] M. G. Khafagy, M. Alouini, and S. Assa, "Full-Duplex Relay Selection in Cognitive Underlay Networks," *IEEE Trans. Commun.*, vol. 66, no. 10, pp. 4431–4443, 2018.

[42] P. D. Diamantoulakis, K. N. Pappi, Z. Ma, X. Lei, P. C. Sofotasios, and G. K. Karagiannidis, "Airborne Radio Access Networks with Simultaneous Lightwave Information and Power Transfer (SLIPT)," in *2018 IEEE Global Communications Conference (GLOBECOM)*, 2018, pp. 1–6.

[43] K. Kumar and D. K. Borah, "Quantize and Encode Relaying Through FSO and Hybrid FSO/RF Links," *IEEE Trans. Veh. Technol*, vol. 64, no. 6, pp. 2361–2374, 2015.

[44] Z. Ghassemlooy, W. Popoola, and S. Rajbhandari, *Optical Wireless Communications: System and Channel Modelling with MATLAB*. CRC Press, 2012.

[45] A. Lapidoth, S. M. Moser, and M. A. Wigger, "On the Capacity of Free-Space Optical Intensity Channels," *IEEE Trans. Inf. Theory*, vol. 55, no. 10, pp. 4449–4461, 2009.

[46] Z. Ding, Z. Yang, P. Fan, and H. V. Poor, "On the Performance of Non-Orthogonal Multiple Access in 5G Systems with Randomly Deployed Users," *IEEE Signal Process. Lett.*, vol. 21, no. 12, pp. 1501–1505, 2014.
[47] J. M. Kahn and J. R. Barry, "Wireless Infrared Communications," *Proc. IEEE*, vol. 85, no. 2, pp. 265–298, 1997.
[48] M. Alouini and A. J. Goldsmith, "Area spectral efficiency of cellular mobile radio systems," *IEEE Trans. Veh. Technol.*, vol. 48, no. 4, pp. 1047–1066, 1999.
[49] G. Pan, J. Ye, and Z. Ding, "Secure Hybrid VLC-RF Systems With Light Energy Harvesting," *IEEE Trans. Commun.*, vol. 65, no. 10, pp. 4348–4359, 2017.
[50] A. P. Prudnikov, Y. A. Brychkov, and O. I. Marichev, *Integrals and Series*. CRC Press, 1992.
[51] J. Men, J. Ge, and C. Zhang, "Performance Analysis of Nonorthogonal Multiple Access for Relaying Networks Over Nakagami-m Fading Channels," *IEEE Trans. Veh. Technol.*, vol. 66, no. 2, pp. 1200–1208, 2017.
[52] A. Goldsmith, *Wireless Communications*. Cambridge University Press, 2005.
[53] Z. Lin and Z. Bai, *Probability Inequalities*. Science Press, 2010.

Yue Xiao received the B.Sc. degree in communication engineering from Southwest Jiaotong University, Chengdu, China, in 2014, where she is currently pursuing the Ph.D. degree. She was a Visitor Researcher with the Wireless Communications Systems Group (WCSG), Aristotle University of Thessaloniki (AUTH). Her research interests include visible light communications, multiple access, channel coding, and cooperative communications.

Panagiotis D. Diamantoulakis (SM18) received the Diploma (five years) and Ph.D. degrees from the Department of Electrical and Computer Engineering, Aristotle University of Thessaloniki (AUTH), Greece, in 2012 and 2017, respectively. From 2017 to 2019, he was a Visiting Post-Doctoral Researcher with the Key Laboratory of Information Coding and Transmission, Southwest Jiaotong University, China, and the Telecommunications Laboratory (LNT), Institute for Digital Communications (IDC), Friedrich-Alexander-Universitt Erlangen-Nrnberg (FAU), Germany. Since 2017, he has been a Post-Doctoral Fellow with the Wireless Communications Systems Group (WCSG), AUTH. His current research interests include resource allocation in optical wireless communications, optimization theory and applications, game theory, non-orthogonal multiple access, and wireless power transfer. He serves as an Editor for *IEEE Wireless Communications Letters*, *Physical Communications* (Elsevier), and *IEEE Open Journal of the Communications Society*. He was also an Exemplary Reviewer of *IEEE Communications Letters* in 2014 and *IEEE Transactions on Communications* in 2017 (top 3% of reviewers).

Zequn Fang received the B.Sc. degree in information and communication engineering from Southwest Jiaotong University, Chengdu, China, in 2014, where he is currently pursuing the Ph.D. degree. His research interests includes information theory, coding, signal process, and wireless communication.

Zheng Ma (M'07) received the B.Sc. and Ph.D. degrees in communications and information system from Southwest Jiaotong University in 2000 and 2006, respectively. He was a Visiting Scholar with the University of Leeds, U.K., in 2003. In 2003 and 2005, he was a Visiting Scholar with The Hong Kong University of Science and Technology. From 2008 to 2009, he was a Visiting Research Fellow with the Department of Communication Systems, Lancaster University, U.K. He is currently a Professor with Southwest Jiaotong University, and also serves as the Deputy Dean with the School of Information Science and Technology. His research interests include: information theory and coding, signal design and applications, FPGA/DSP implementation, and professional mobile radio. He has authored over 120 research papers in high quality journals and conferences. He is currently the Senior Editor of the *IEEE Communications Letters*. He is also the Vice-Chairman of Information Theory Chapter in the IEEE Chengdu section. He received the Marie Curie Individual Fellowship in 2018.

Li Hao received her Ph.D. degree in Transportation Information Engineering and Controlling from Southwest Jiaotong University, China, in 2003. She is currently the professor and dean with the School of Information Science and Technology, Southwest Jiaotong University. Her research interests include information theory & coding, 5G/B5G communications, cooperative communications, and low-power IoT communications. She is currently the deputy director of communication and signaling branch of China Railway Society.

George K. Karagiannidis (M'96-SM'03-F'14) was born in Pithagorion, Samos Island, Greece. He received the University Diploma (5 years) and PhD degree, both in electrical and computer engineering from the University of Patras, in 1987 and 1999, respectively. From 2000 to 2004, he was a Senior Researcher at the Institute for Space Applications and Remote Sensing, National Observatory of Athens, Greece. In June 2004, he joined the faculty of Aristotle University of Thessaloniki, Greece where he is currently Professor in the Electrical & Computer Engineering Dept. and Director of Digital Telecommunications Systems and Networks Laboratory. He is also Honorary Professor at Southwest Jiaotong University, Chengdu, China.

His research interests are in the broad area of Digital Communications Systems and Signal processing, with emphasis on Wireless Communications, Optical Wireless Communications, Wireless Power Transfer and Applications, Molecular and Nanoscale Communications, Stochastic Processes in Biology and Wireless Security.

He is the author or co-author of more than 400 technical papers published in scientific journals and presented at international conferences. He is also author of the Greek edition of a book on "Telecommunications Systems" and co-author of the book "Advanced Optical Wireless Communications Systems", Cambridge Publications, 2012.

Dr. Karagiannidis has been involved as General Chair, Technical Program Chair and member of Technical Program Committees in several IEEE and non-IEEE conferences. In the past, he was Editor in *IEEE Transactions on Communications*, Senior Editor of *IEEE Communications Letters*, Editor of the *EURASIP Journal of Wireless Communications & Networks* and several times Guest Editor in *IEEE Selected Areas in Communications*. From 2012 to 2015 he was the Editor-in Chief of *IEEE Communications Letters*.

Dr. Karagiannidis is one of the highly-cited authors across all areas of Electrical Engineering, recognized from Clarivate Analytics as Web-of-Science Highly-Cited Researcher in the five consecutive years 2015-2019.